

Self-energy corrections in an antiferromagnet — interplay of classical and quantum effects on quasiparticle dispersion

Pooja Srivastava and Avinash Singh*
Department of Physics, Indian Institute of Technology Kanpur - 208016

Self-energy corrections due to fermion-magnon interaction are studied in the antiferromagnetic state of the $t - t' - t''$ Hubbard model within the rainbow (noncrossing) approximation in the full U range from weak to strong coupling. The role of classical (mean-field) features of fermion and magnon dispersion, associated with finite U, t', t'' , are examined on quantum corrections to quasiparticle energy, weight, one-particle density of states etc. A finite- U induced classical dispersion term, absent in the $t - J$ model, is found to play an important role in suppressing the quasiparticle weight for states near $\mathbf{k} = (0, 0)$, as seen in cuprates. For intermediate U , the renormalized AF band gap is found to be nearly half of the classical value, and the weak coupling limit is quite non-trivial due to strongly suppressed magnon amplitude. For finite t' , the renormalized AF band gap is shown to vanish at a critical interaction strength U_c , yielding a spin fluctuation driven first-order AF insulator - PM metal transition. Quasiparticle dispersion evaluated with the same set of Hubbard model cuprate parameters, as obtained from a recent magnon spectrum fit, provides excellent agreement with ARPES data for $\text{Sr}_2\text{CuO}_2\text{Cl}_2$.

I. INTRODUCTION

Driven by the intensive effort to understand the fascinating properties of doped cuprates, substantial theoretical progress has been made in recent years in the area of correlated electron systems. In particular, the study of quantum spin fluctuations in the antiferromagnetic (AF) state and the renormalization of quasiparticle properties of doped carriers due to coupling with spin fluctuations has attracted much attention in the context of antiferromagnetic spin correlations, anomalous normal state properties, spin-fluctuation mediated pairing, optical conductivity etc.¹

Photoemission studies of quasiparticle energies in $\text{Sr}_2\text{CuO}_2\text{Cl}_2$ have revealed^{2,3} that the energy difference between the $\mathbf{k} = (\pi/2, \pi/2)$ and $(\pi, 0)$ states cannot be understood within the $t - J$ model, and by including additional next-nearest-neighbour (NNN) and NNNN hopping terms t' and t'' , improved fittings have been obtained within the $t - t' - t'' - J$ model in the Born approximation^{4,5,6,7,8,9,10,11} and the $t - t' - t''$ Hubbard model at the mean-field level,^{12,13} and within Born approximation.¹⁴ The t' and t'' dispersion terms control the $(0, 0) - (\pi, 0)$ and $(0, 0), (\pi, 0) - (\pi/2, \pi/2)$ energy separations respectively, and are thus crucial for quasiparticle dispersion fitting in cuprates. The need for more realistic microscopic models for cuprates which include additional hopping terms has also been acknowledged recently from band structure, photoemission, and neutron-scattering studies of high- T_c and related materials.^{15,16,17,18,19,20} Estimates for $|t'/t|$ range from 0.15 to 0.5.

Recent high-resolution inelastic neutron scattering studies of the spin-wave spectrum of the square-lattice spin-1/2 antiferromagnet La_2CuO_4 have revealed noticeable spin-wave dispersion along the AF zone boundary.²¹ While the simplest explanation for the observed spin-wave dispersion is in terms of a ferromagnetic NNN spin

coupling J' , it was pointed out^{21,22} that a more natural explanation can be obtained in terms of the one-band Hubbard model, for which the strong coupling expansion in powers of t/U generates extended-range spin couplings. Fits of the spin-wave spectrum yield $t \approx 0.35$ eV and $U/t \approx 7$, with $|t'|/t = 0.25$.^{21,22}

It is therefore of interest to study the role of additional spin couplings generated in the finite- U Hubbard model on quasiparticle dispersion. In this paper we study the fermion self energy due to fermion-magnon interaction in the $t - t' - t''$ Hubbard model, and examine the interplay between classical (mean-field) features of fermion and magnon dispersion and quantum (self-energy) corrections on quasiparticle dispersion. The $t - t'$ Hubbard model also provides a concrete realization of a stable doped antiferromagnetic state,^{12,23} characterized by magnon damping due to decay into particle-hole excitations across the Fermi energy,²⁴ thus allowing for finite doping studies.

The interplay between classical and quantum effects is manifested in several ways. For example, the AF state of the Hubbard model at strong coupling involves a mean-field dispersion term $4J\gamma_{\mathbf{k}}^2$, where $J = 4t^2/U$ and $\gamma_{\mathbf{k}} = (\cos k_x + \cos k_y)/2$. Absent in the $t - J$ model, this large classical dispersion term has an energy scale twice that of the magnon energy, and therefore quasiparticle renormalizations in the Hubbard and $t - J$ models are expected to differ with increasing J . Furthermore, the finite- U induced dispersion term $4J\gamma_{\mathbf{k}}^2$ intrinsically contains effective NNN ($t' = J/2$) and NNNN ($t'' = J/4$) hopping terms, and these finite- U contributions are entangled with the physical hopping strengths in the t' and t'' values determined by quasiparticle dispersion fitting for cuprates within the $t - t' - t'' - J$ model.

Another manifestation of the interplay is a competition between classical and quantum effects. Thus, while quantum correction lowers the hole energy near $(\pi/2, \pi/2)$ in the $t - J$ and Hubbard models, the dispersion term $-4t' \cos k_x \cos k_y$ favours the $(\pi, 0)$ state (for positive t').

An effective one dimensional dispersion can thus result from a net cancellation of the dispersion along the magnetic zone boundary.

An instance where both classical and quantum effects come together involves the AF band gap for particle-hole excitations. Both, the classical dispersion term $-4t \cos k_x \cos k_y$ and the quantum correction, reduce the band gap significantly, which may therefore be expected to vanish at a moderate U value. The antiferromagnetic insulator - paramagnetic metal transition associated with the vanishing band gap, relevant for transition-metal oxides such as V_2O_3 , can thus be explored within a spin-fluctuation theory.

Competition between the two classical dispersion terms in the $t - t' - t''$ Hubbard model introduces asymmetry in the two AF bands, in terms of bandwidth and density of states. The self-energy corrections for added holes and electrons are therefore expected to be significantly different. Indeed, we find a dramatically enhanced strong-coupling signature in the self-energy correction for the narrow band.

After a brief review of the mean-field AF state of the $t - t' - t''$ Hubbard model (section II), the self energy for one added hole (electron) is obtained in the rainbow approximation (section III). Various quasiparticle properties are evaluated for the Hubbard model in the full U range (section IV). The role of finite t' and t'' is studied in section V, and our conclusions are presented in section VI. Some general features associated with the self energy in the AF state are put in Appendix A, and the contrasting case of undoped AF state is provided in Appendix B.

II. MEAN-FIELD AF STATE OF THE $t - t' - t''$ HUBBARD MODEL

To introduce the notation, we briefly review the mean-field (Hartree-Fock) state of the Hubbard model

$$H = \sum_{i,\delta,\sigma} -t_\delta a_{i,\sigma}^\dagger a_{i+\delta,\sigma} + U \sum_i n_{i\uparrow} n_{i\downarrow} \quad (1)$$

on a square lattice, with hopping terms $t_\delta = t, t',$ and t'' , connecting NN, NNN, and NNNN pairs of sites $(i, i + \delta)$, respectively. It is convenient to use the two-sublattice basis as translational symmetry is preserved, and the Hartree-Fock (HF) Hamiltonian

$$H_0^\sigma(\mathbf{k}) = (\epsilon'_\mathbf{k} + \epsilon''_\mathbf{k}) \mathbf{1} + \begin{bmatrix} -\sigma\Delta & \epsilon_\mathbf{k} \\ \epsilon_\mathbf{k} & \sigma\Delta \end{bmatrix} \quad (2)$$

for spin σ , in terms of the free-particle energies $\epsilon_\mathbf{k} = -2t(\cos k_x + \cos k_y)$, $\epsilon'_\mathbf{k} = -4t' \cos k_x \cos k_y$, and $\epsilon''_\mathbf{k} = -2t''(\cos 2k_x + \cos 2k_y)$. Here $2\Delta = mU$, where m is the sublattice magnetization.

For the classical level (mean-field) fermion propagator,

$$[G_\uparrow^0(\mathbf{k}, \omega)] = \frac{\begin{bmatrix} \alpha_\mathbf{k}^2 & -\alpha_\mathbf{k}\beta_\mathbf{k} \\ -\alpha_\mathbf{k}\beta_\mathbf{k} & \beta_\mathbf{k}^2 \end{bmatrix}}{\omega - E_\mathbf{k}^\ominus - i\eta} + \frac{\begin{bmatrix} \beta_\mathbf{k}^2 & \alpha_\mathbf{k}\beta_\mathbf{k} \\ \alpha_\mathbf{k}\beta_\mathbf{k} & \alpha_\mathbf{k}^2 \end{bmatrix}}{\omega - E_\mathbf{k}^\oplus + i\eta} \quad (3)$$

for spin \uparrow , and $[G_\downarrow^0(\mathbf{k}, \omega)] = [\sigma_x][G_\uparrow^0(\mathbf{k}, \omega)][\sigma_x]$ from spin-sublattice symmetry, where $[\sigma_x] = \begin{bmatrix} 0 & 1 \\ 1 & 0 \end{bmatrix}$. While the AF band energies

$$\begin{aligned} E_\mathbf{k}^\ominus &= (\epsilon'_\mathbf{k} + \epsilon''_\mathbf{k}) - (\Delta^2 + \epsilon_\mathbf{k}^2)^{1/2} \\ E_\mathbf{k}^\oplus &= (\epsilon'_\mathbf{k} + \epsilon''_\mathbf{k}) + (\Delta^2 + \epsilon_\mathbf{k}^2)^{1/2}, \end{aligned} \quad (4)$$

for the lower and upper bands are modified by t' and t'' , the fermion amplitudes $|\mathbf{k}\rangle \equiv (a_\mathbf{k} \ b_\mathbf{k})$ remain unchanged:

$$\begin{aligned} \alpha_\mathbf{k}^2 &= \frac{1}{2} \left(1 + \frac{\Delta}{\sqrt{\Delta^2 + \epsilon_\mathbf{k}^2}} \right) \\ \beta_\mathbf{k}^2 &= \frac{1}{2} \left(1 - \frac{\Delta}{\sqrt{\Delta^2 + \epsilon_\mathbf{k}^2}} \right). \end{aligned} \quad (5)$$

In the strong coupling limit ($U \gg t$), the majority and minority densities reduce to $1 - \epsilon_\mathbf{k}^2/U^2$ and $\epsilon_\mathbf{k}^2/U^2$.

Similarly, for the magnon propagator we have

$$[\chi^{-+}(\mathbf{q}, \Omega)] = \frac{\begin{bmatrix} v_\mathbf{q}^2 & u_\mathbf{q}v_\mathbf{q} \\ u_\mathbf{q}v_\mathbf{q} & u_\mathbf{q}^2 \end{bmatrix}}{\Omega - \Omega_\mathbf{q} + i\eta} + \frac{\begin{bmatrix} u_\mathbf{q}^2 & u_\mathbf{q}v_\mathbf{q} \\ u_\mathbf{q}v_\mathbf{q} & v_\mathbf{q}^2 \end{bmatrix}}{\Omega + \Omega_\mathbf{q} - i\eta} \quad (6)$$

at the classical (ladder-sum) level. For the Hubbard model in the strong coupling limit the magnon amplitudes $|\mathbf{q}\rangle \equiv (u_\mathbf{q} \ v_\mathbf{q})$ and energy $\Omega_\mathbf{q}$ are given by^{25,26}

$$\begin{aligned} u_\mathbf{q}^2 &= \left(1/\sqrt{1 - \gamma_\mathbf{q}^2} + 1 \right) / 2 \\ v_\mathbf{q}^2 &= \left(1/\sqrt{1 - \gamma_\mathbf{q}^2} - 1 \right) / 2 \\ u_\mathbf{q}v_\mathbf{q} &= \left(-\gamma_\mathbf{q}/\sqrt{1 - \gamma_\mathbf{q}^2} \right) / 2 \\ \Omega_\mathbf{q} &= 2J\sqrt{1 - \gamma_\mathbf{q}^2} \end{aligned} \quad \text{where } \gamma_\mathbf{q} = (\cos q_x + \cos q_y)/2. \quad (7)$$

III. SELF ENERGY IN THE RAINBOW APPROXIMATION

We now obtain the self energy due to fermion-magnon interaction in the rainbow approximation (Fig. 1), in which all noncrossing diagrams are summed, representing multiple magnon emission and absorption processes. The magnon lines are considered here at the classical (ladder-sum) level. The first-order quantum corrections to magnon propagator yield momentum-independent renormalizations of the magnon amplitude and energy in the strong coupling limit,²⁷ which can be incorporated easily.

The rainbow self-energy correction

$$[\Sigma(\mathbf{k}, \omega)] = U^2 \sum_{\mathbf{q}} \int \frac{d\Omega}{2\pi i} [\chi^{-+}(\mathbf{q}, \Omega)] [G_\downarrow(\mathbf{k} - \mathbf{q}, \omega - \Omega)] \quad (8)$$

for state $|\mathbf{k}\uparrow\rangle$ involves the renormalized propagator for state $|\mathbf{k} - \mathbf{q}\downarrow\rangle$. However, from spin-sublattice symmetry,

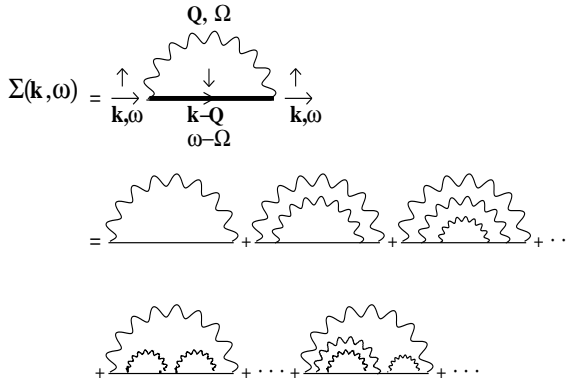


FIG. 1: Self energy in the rainbow (noncrossing) approximation. Wavy lines represent the magnon propagator. The bare fermion-magnon interaction vertex is U .

the fermion propagators are identical if their spin and sublattice indices are simultaneously switched, so that

$$\begin{aligned} [G_{\downarrow}(\mathbf{k} - \mathbf{q}, \omega - \Omega)] &= [\sigma_x][G_{\uparrow}(\mathbf{k} - \mathbf{q}, \omega - \Omega)][\sigma_x] \\ &= \frac{[\sigma_x][\mathbf{k} - \mathbf{q}]\langle \mathbf{k} - \mathbf{q} | [\sigma_x]}{\omega - \Omega - E_{\mathbf{k}-\mathbf{q}}^0 - \Sigma_{\mathbf{k}-\mathbf{q}}(\omega - \Omega)}, \end{aligned} \quad (9)$$

using Eq. (A1). The above replacement in Eq. (8) thus yields a self-consistent equation for the fermion self energy $\Sigma_{\mathbf{k}}(\omega)$ which is independent of spin.

A. One hole (electron) in the AF

The situation is simplest for a single hole introduced in a filled lower AF band, as the available scattering states $|\mathbf{k} - \mathbf{q}\rangle$ span all of the lower AF band. For finite doping, hole states already occupied must be excluded from the scattering process. From particle-hole symmetry, the situation is symmetrical for an added electron to the empty upper band, under sign change of t' and t'' .

The motion of a hole in an antiferromagnetic background has been studied extensively in the recent past.¹ The string of upturned spins and broken antiferromagnetic bonds left in its wake renders the hole motion highly incoherent, and the description of the hole carrying along the locally scrambled AF spin arrangement is a highly nontrivial many-body theoretical problem.

Several aspects of the hole propagator, such as the spectral function, quasiparticle dispersion, bandwidth and weight, have been studied for the $t - J$ model within the rainbow (noncrossing) approximation,^{28,29,30,31,32,33} also called the self-consistent Born approximation (SCBA). Comparison with exact diagonalization results³⁴ show the SCBA results to be in good agreement for small J , and contributions of crossing diagrams have been argued to be small.³¹

We will show that the self energy expression for the Hubbard model, obtained via the formally weak-

coupling, many-body perturbation-theoretic expansion in powers of U , when carried to the strong coupling limit ($U/t \rightarrow \infty$), reduces exactly to the SCBA result for the $t - J$ model, apart from a classical dispersion term, absent in the $t - J$ model. Similar exact correspondence has been pointed out for magnon dispersion, both at the classical level and including quantum corrections, sublattice magnetization, ground-state energy, two-magnon Raman scattering etc.

As $G_{\downarrow}(\mathbf{k} - \mathbf{q}, \omega - \Omega)$ in Eq. (8) is an advanced propagator, representing scattering states for the added hole, the Ω integral (replaced by a contour integral over the upper half plane) picks a contribution only from the advanced part of the magnon propagator given in Eq. (6). It is convenient to introduce a composite amplitude

$$|\sigma(\mathbf{k}, \mathbf{q})\rangle = |\mathbf{q}\rangle \times [\sigma_x]|\mathbf{k} - \mathbf{q}\rangle = \begin{pmatrix} u_{\mathbf{q}} & \beta_{\mathbf{k}-\mathbf{q}} \\ v_{\mathbf{q}} & \alpha_{\mathbf{k}-\mathbf{q}} \end{pmatrix}, \quad (10)$$

for the magnon-hole interaction vertex, in terms of which we obtain for the hole self energy

$$\begin{aligned} \Sigma_{\mathbf{k}}(\omega) &\equiv \langle \mathbf{k} | [\Sigma(\mathbf{k}, \omega)] | \mathbf{k} \rangle = (\alpha_{\mathbf{k}}^* \beta_{\mathbf{k}}^*) [\Sigma(\mathbf{k}, \omega)] \begin{pmatrix} \alpha_{\mathbf{k}} \\ \beta_{\mathbf{k}} \end{pmatrix} \\ &= U^2 \sum_{\mathbf{q}} \frac{\langle \mathbf{k} | \sigma(\mathbf{k}, \mathbf{q}) \rangle \langle \sigma(\mathbf{k}, \mathbf{q}) | \mathbf{k} \rangle}{\omega + \Omega_{\mathbf{q}} - E_{\mathbf{k}-\mathbf{q}}^{\ominus} - \Sigma_{\mathbf{k}-\mathbf{q}}(\omega + \Omega_{\mathbf{q}})} \\ &= U^2 \sum_{\mathbf{q}} \frac{(\alpha_{\mathbf{k}} u_{\mathbf{q}} \beta_{\mathbf{k}-\mathbf{q}} + \beta_{\mathbf{k}} v_{\mathbf{q}} \alpha_{\mathbf{k}-\mathbf{q}})^2}{\omega + \Omega_{\mathbf{q}} - E_{\mathbf{k}-\mathbf{q}}^{\ominus} - \Sigma_{\mathbf{k}-\mathbf{q}}(\omega + \Omega_{\mathbf{q}})}. \end{aligned} \quad (11)$$

The above yields a self-consistent equation for the hole self energy in the form of an integral equation, which describes the hole renormalization due to multiple magnon emission and absorption processes, as it moves in the AF background. Within the rainbow approximation, Eq. (11) is valid for arbitrary U , in the whole range from weak to strong coupling, and for extended-range hopping terms. As the self energy depends on the classical dispersion, explicitly through $E_{\mathbf{k}-\mathbf{q}}^{\ominus}$ and implicitly through the magnon energy $\Omega_{\mathbf{q}}$, an interesting interplay is expected between classical and quantum effects on quasiparticle energies.

IV. SELF ENERGY FOR THE HUBBARD MODEL

A. Strong coupling limit

We now consider the rainbow self energy for the Hubbard model in the analytically simple strong coupling limit ($U/t \rightarrow \infty$), and compare with the $t - J$ model results. We write the classical (mean-field) hole energy

$$E_{\mathbf{k}}^{\ominus} = -\sqrt{\Delta^2 + \epsilon_{\mathbf{k}}^2} \approx -\Delta - 4J_c \gamma_{\mathbf{k}}^2 \quad (12)$$

where a classical energy scale $J_c = 4t^2/U$ has been introduced to distinguish the classical dispersion term $4J_c \gamma_{\mathbf{k}}^2$

generated in the Hubbard model at strong coupling. Substituting in Eq. (11) the fermion and magnon amplitudes and energies from Eqs. (5), (7), and (12), and shifting the energy by Δ to bring the zero of the energy scale to the lower band edge, the self energy is compactly written as

$$\Sigma_{\mathbf{k}}(\omega) = t^2 z^2 \sum_{\mathbf{q}} \frac{(u_{\mathbf{q}} \gamma_{\mathbf{k}-\mathbf{q}} + v_{\mathbf{q}} \gamma_{\mathbf{k}})^2}{\omega + \Omega_{\mathbf{q}} + 4J_c \gamma_{\mathbf{k}-\mathbf{q}}^2 - \Sigma_{\mathbf{k}-\mathbf{q}}(\omega + \Omega_{\mathbf{q}})} . \quad (13)$$

The above self energy introduces a quantum correction to the classical (mean-field) hole dispersion. Apart from the classical dispersion term J_c in the denominator, the above self-energy expression reduces exactly to the SCBA result for the $t - J$ model.^{28,29,30}

B. Strong-coupling results

The self-consistent numerical evaluation of the self energy was carried out using a 52×52 grid in \mathbf{k} space, and a frequency interval $\Delta\omega = 0.1$ for ω in the range $-10 < \omega < 10$. The self energy was iteratively evaluated, starting with $\Sigma_{\mathbf{k}}(\omega) = 0$. Typically, self-consistency was achieved within ten iterations. For $J_c = 0$, our numerical results are in exact agreement with the $t - J$ model results of Liu and Manousakis.³¹

The hole self-energy variation with successive iterations, shown in Fig. 2, effectively illustrates the role of multiple magnon emission and absorption processes. The first iteration yields the single magnon contribution, and successive iterations incorporate higher-order magnon processes. The significant difference, especially for $J \ll t$, between the first-order and the self-consistent results, indicates the relative importance of multi-magnon processes.

From Eq. (A1), intersection of $\omega - E_{\mathbf{k}}^{\ominus}$ with $\text{Re } \Sigma_{\mathbf{k}}(\omega)$ yields the renormalized quasiparticle energy $E_{\mathbf{k}}^*$ where the spectral function peaks, as shown in Fig. 3 for $\mathbf{k} = (\frac{\pi}{2}, \frac{\pi}{2})$. The quadratic growth of $\text{Im } \Sigma_{\mathbf{k}}(\omega)$ near $\omega \approx E_{\mathbf{k}}^*$ is due to the long-wavelength magnon modes. In Eq. (13), neglecting the weak q^2 dependence of $\gamma_{\mathbf{k}-\mathbf{q}}$ and $\Sigma_{\mathbf{k}-\mathbf{q}}$ in comparison with the linear dependence $\Omega_{\mathbf{q}} = \sqrt{2}Jq$ of the magnon energy for small q , one obtains

$$\begin{aligned} \text{Im } \Sigma_{\mathbf{k}}(\omega) &\sim t^2 z^2 \int q dq (1/q) (q_x + q_y)^2 \delta(\omega + \Omega_{\mathbf{q}} + \text{Re } \Sigma_{\mathbf{k}}) \\ &\sim (\omega + E_{\mathbf{k}}^*)^2 . \end{aligned} \quad (14)$$

Magnon damping at finite doping due to intraband particle-hole excitations is therefore expected to be important for quasiparticle damping.

The large classical term $4J_c \gamma_{\mathbf{k}}^2$ suppresses the self-energy correction in Eq. (13), in addition to providing dispersion at the mean-field level, and these combined effects of J_c on quasiparticle dispersion are discussed below. Figure 4 shows the quasiparticle dispersion along different symmetry directions for $J = 0.5$.

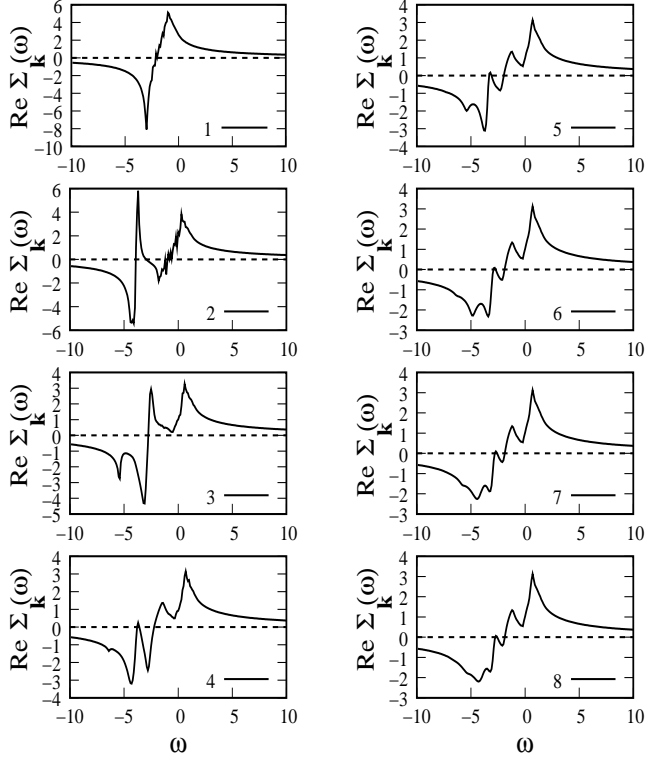


FIG. 2: Variation of self energy with iterations, effectively illustrating the role of successively higher-order magnon processes. Here $J = 0.5$ and $\mathbf{k} = (\pi/2, \pi/2)$.

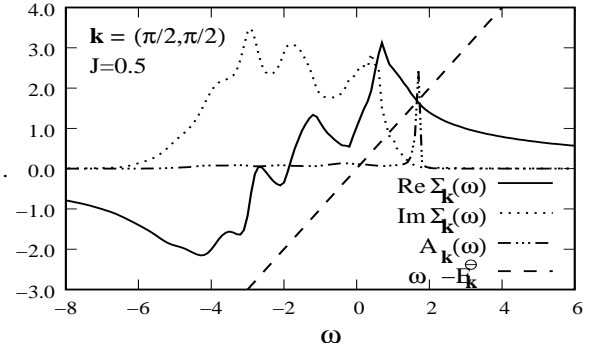


FIG. 3: The hole spectral function $A_{\mathbf{k}}(\omega)$ shows the quasiparticle peak at the intersection of $\omega - E_{\mathbf{k}}^{\ominus}$ with $\text{Re } \Sigma_{\mathbf{k}}(\omega)$.

Here the quasiparticle energies are obtained from the peak in the spectral function $A_{\mathbf{k}}(\omega)$ occurring at lowest hole energy. The small dispersion developed along the M - M' direction (magnetic zone boundary) is purely quantum mechanical. The substantially different curvatures at $\mathbf{k} = (\pi/2, \pi/2)$ along the $\Gamma - X$ and M - M' directions shows a highly anisotropic quasiparticle dispersion with different effective masses. The quasiparticle

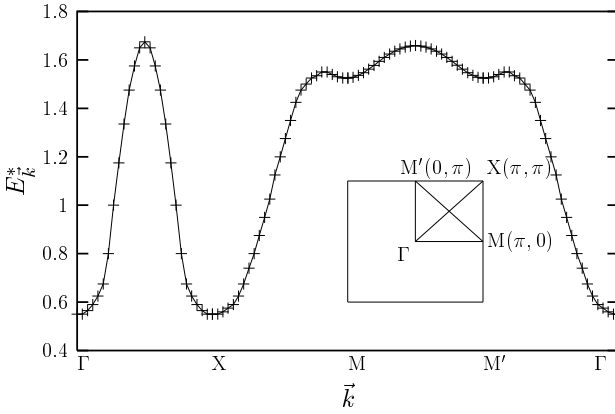


FIG. 4: Quasiparticle dispersion along different symmetry directions, for $J = 0.5$.

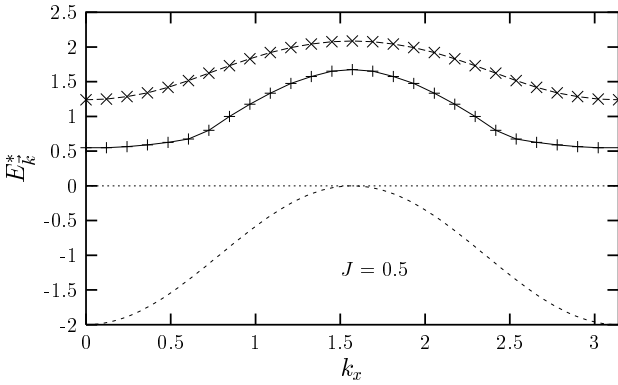


FIG. 5: Quasiparticle dispersion along the Γ – X direction with (+) and without (x) the classical dispersion term J_c , along with the mean-field dispersion.

energy is maximum for $\mathbf{k} = (\pi/2, \pi/2)$.

Figure 5 shows a comparison of the quasiparticle dispersion along the Γ – X direction with and without J_c , providing a comparison with the SCBA results for the t – J model ($J_c = 0$). The classical dispersion term J_c reduces the quasiparticle energy renormalization, and significantly flattens the dispersion near the Γ and X points, and also increases the quasiparticle bandwidth. Furthermore, for $\mathbf{k} = (0, 0)$, the spectral weight of the highest-energy peak (lowest-energy for hole) is drastically reduced by J_c , in sharp contrast with the $J_c = 0$ case, as shown in Fig. 6. This finite- U induced feature is quite significant with regard to photoemission studies of cuprates, where the $\mathbf{k} = (0, 0)$ peak is seen to be extremely weak in comparison with $(\pi/2, \pi/2)$.

The enhancement in the self-energy correction with decreasing magnon energy scale (J) is seen in Fig. 7, both through (a) decreasing quasiparticle weight for $\mathbf{k} = (\pi/2, \pi/2)$ signifying enhancement in incoherent part due to multi-magnon processes, and (b) increasing quasiparticle energy renormalization. Comparison with the t – J model results ($J_c = 0$) illustrates the increasing suppression of quantum correction by the classical dispersion term with J .

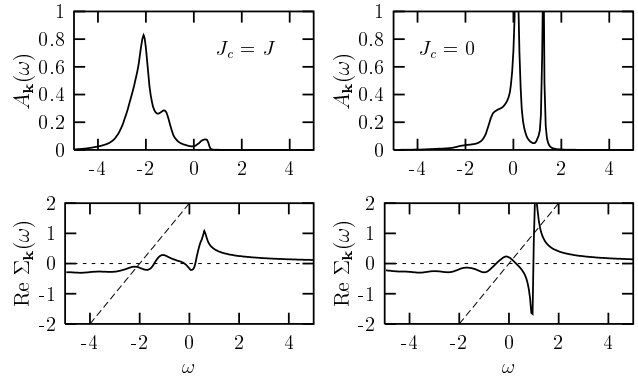


FIG. 6: The $\mathbf{k} = (0, 0)$ spectral function is significantly modified by the finite- U induced classical dispersion term J_c , as shown in terms of the intersection of $\text{Re } \Sigma_{\mathbf{k}}(\omega)$ with the line $\omega + 4J_c \gamma_{\mathbf{k}}^2$. Here $J = 0.5$.

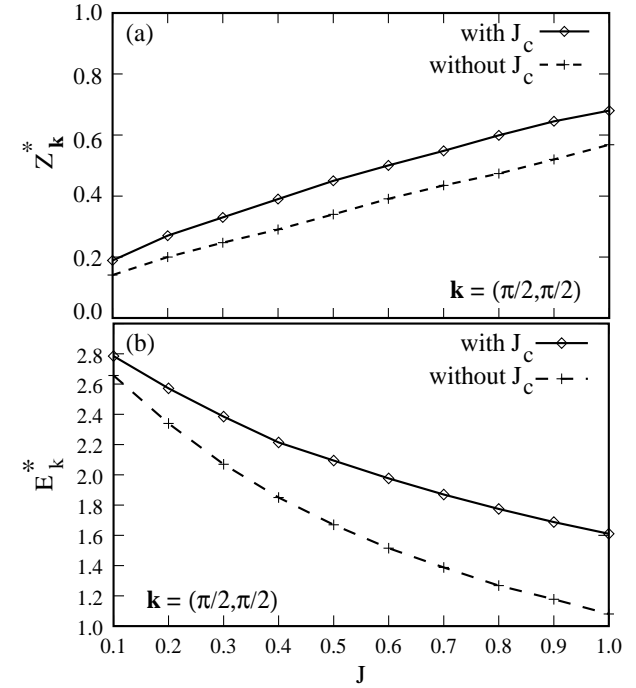


FIG. 7: Comparison of quasiparticle weight $Z_{\mathbf{k}}$ and energy $E_{\mathbf{k}}^*$ with and without J_c , showing increasing differences with J .

tion of quantum correction by the classical dispersion term with J .

C. Intermediate and weak coupling

Self energy for finite U is of special interest as several additional features of the AF state can be explored. These include one-particle density of states for both bands, renormalized band gap, and the possibility of van-

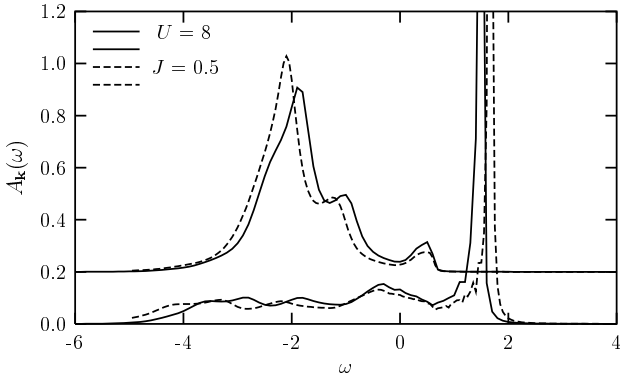


FIG. 8: Comparison of strong-coupling and finite- U spectral functions for $\mathbf{k} = (\pi/2, \pi/2)$ and $(0, 0)$.

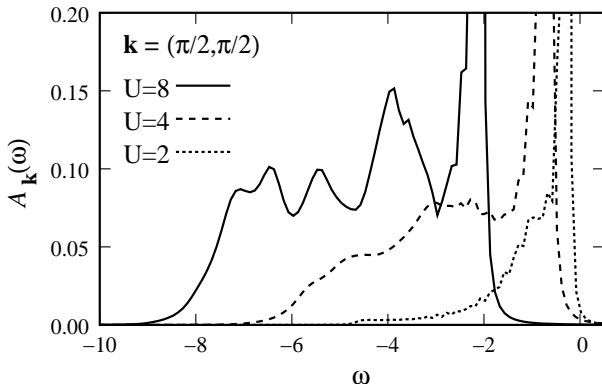


FIG. 9: Increasingly incoherent hole spectral function with increasing U , for $\mathbf{k} = (\pi/2, \pi/2)$.

ishing band gap and a metal-insulator transition driven by spin fluctuations. Furthermore, the magnon nature is qualitatively modified at finite U , as studied earlier in detail in the intermediate,³⁵ and weak³⁶ coupling limits. Extended-range spin couplings generated at intermediate U remove the degeneracy in the magnon spectrum along the AF zone boundary. Also, the decreasing AF band gap 2Δ begins to play a significant role, and for small U the magnon amplitude is strongly suppressed for modes with energy approaching 2Δ . These features were not explored in earlier SDW-SCBA calculations^{14,37} for the Hubbard model, where only strong coupling expressions for magnon amplitude and energy were employed, and are naturally beyond the scope of the $t - J$ model in which the upper AF band is projected out, and the magnon dispersion corresponds to NN spin coupling only.

For arbitrary U , the hole self energy $\Sigma_{\mathbf{k}}(\omega)$ is determined from Eq. (11), with classical fermion amplitudes and energies taken from Eqs. (4) and (5), and the classical (ladder-sum) magnon energy $\Omega_{\mathbf{q}}$ and amplitudes $u_{\mathbf{q}}$, $v_{\mathbf{q}}$ determined numerically, as described earlier.^{35,36}

Comparison of spectral functions evaluated for inter-

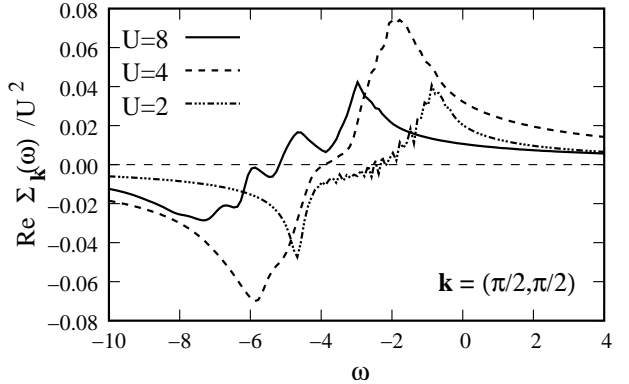


FIG. 10: Approximate U^2 scaling of the real part of self energy, showing a dominant single-magnon contribution with decreasing U .

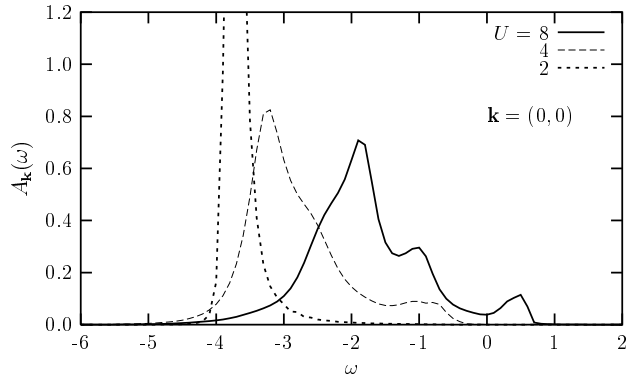


FIG. 11: Evolution of the $\mathbf{k} = (0, 0)$ spectral function with decreasing U .

mediate U with strong coupling results (Fig. 8) shows a noticeable reduction in the quasiparticle bandwidth. With decreasing U , the hole spectral function becomes increasingly coherent (Fig. 9), the self energy approximately scales as U^2 (Fig. 10), and the shape of $\text{Re} \Sigma_{\mathbf{k}}(\omega)$ increasingly resembles the single-magnon result (Fig. 3), indicating dominant lowest-order (U^2) contribution, as expected. Evolution of the $\mathbf{k} = (0, 0)$ spectral function (Fig. 11) shows that the peak at lowest hole energy remains nearly incoherent down to very low U values.

The one-particle (tunneling) density of states is shown in Fig. 12 for $U = 8, 4, 2$ (corresponding to mean-field gaps $2\Delta = 7.2, 2.8, 0.75$), displaying the smooth approach towards the free-particle DOS with decreasing U . The band gap remains finite no matter how small U is. States are pulled within the classical energy gap 2Δ due to the fermion-magnon scattering, and the resulting fermion spectral function incoherence spreads the DOS over a broader frequency range. Pseudo-gap feature appears in the strong coupling limit. These DOS features are in good agreement with exact diagonalization results.³⁴

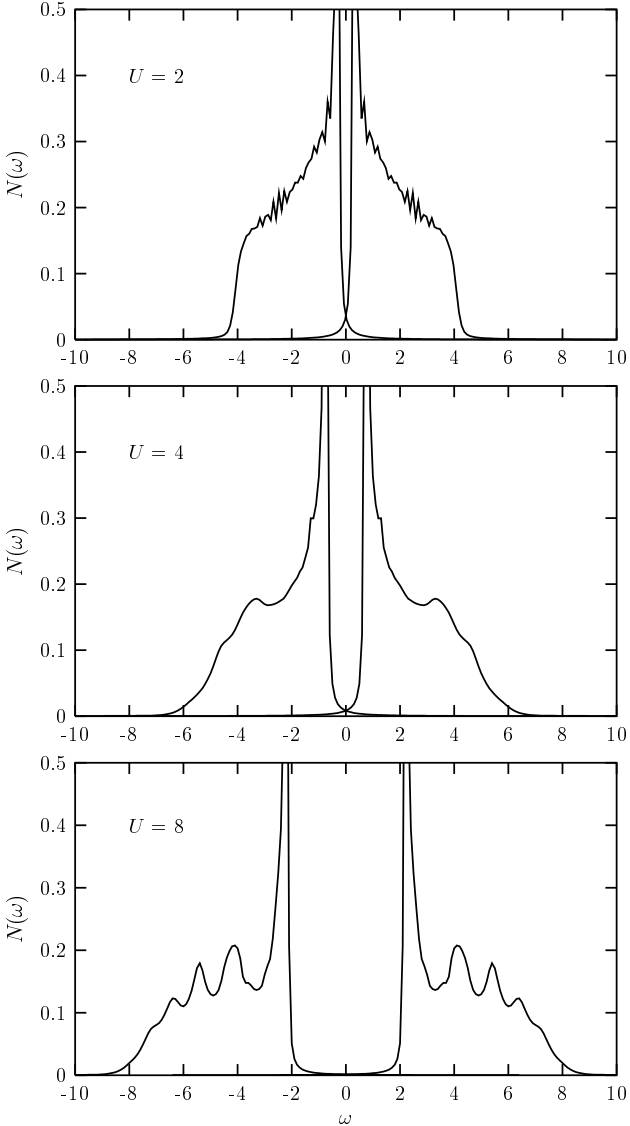


FIG. 12: Renormalized one-particle (tunneling) density of states for $U = 8, 4, 2$.

For all U , the state $\mathbf{k} = (\pi/2, \pi/2)$ continues to be the lowest-energy hole state, and therefore, from particle-hole symmetry, also the lowest-energy electron state in the upper band. The minimum electron-hole pair excitation energy therefore yields the renormalized band gap $E_g = 2|E_{\mathbf{k}}^*|$, with $\mathbf{k} = (\pi/2, \pi/2)$. We find that the ratio E_g^*/E_g^0 is reduced to nearly 1/2 in a broad U range, as shown in Fig. 13, and approaches 1 in both weak and strong coupling limits, although with fundamentally different behaviour. The weak-coupling trend indicates that the band gap remains finite for all U . For $U \geq 8$, we have used the strong-coupling self energy from Eq. (13).

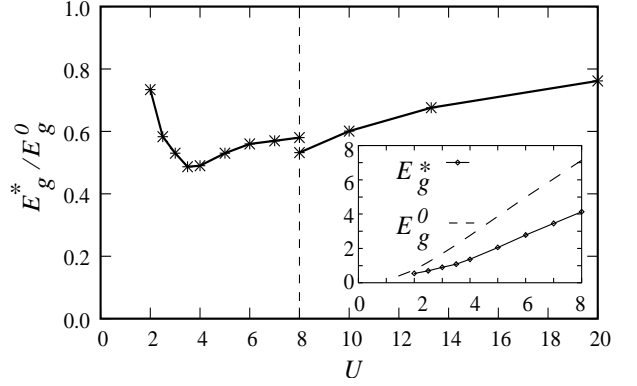


FIG. 13: The ratio E_g^*/E_g^0 of renormalized and classical band gaps is nearly 1/2 for intermediate coupling, and approaches 1 in both weak and strong coupling limits.

V. ROLE OF HOPPING TERMS t', t''

Finite hopping terms t', t'' add an additional dimension to the competition between classical and quantum effects on quasiparticle dispersion. Thus, the classical dispersion term $\epsilon_{\mathbf{k}}$ introduces a dispersion along the MM' direction of the Brillouin zone, renders the two AF bands asymmetrical, yielding narrow and wide bands for a given U value, and also significantly reduces the band gap, making it possible for quantum fluctuation effects to close the gap at a moderate U value. Furthermore, the frustration due to competing AF spin couplings generated by t', t'' leads to magnon softening,³⁸ and the reduced magnon energy scale is expected to enhance the self-energy correction. This frustration effect is absent within the $t - t' - t'' - J$ model having only NN AF spin coupling.

We have evaluated the hole self energy for finite U and positive t' using Eq. (11), with appropriate classical fermion energies and amplitudes given in Eqs. (4) and (5). The quasiparticle energy difference between the $(\pi/2, \pi/2)$ and $(\pi, 0)$ states decreases nearly linearly with t' , and vanishes for $t' \approx 0.1$, resulting in a nearly one dimensional quasiparticle dispersion along the $\Gamma - X$ direction. For higher t' values, the classical effect dominates, and $\mathbf{k} = (\pi, 0)$ is the lowest-energy hole state. From particle-hole symmetry, these results also apply to an added electron in the upper band for negative t' .

Figure 14 shows the one-particle density of states for $t' = 0.5$ and $U \approx 5$. While a substantial classical gap remains, the renormalized band gap is seen to just vanish. However, as the lowest-energy hole and electron states correspond to different momenta — $(\pi, 0)$ for hole and $(\pi/2, \pi/2)$ for electron — the band gap is indirect, yielding a finite optical gap. A further reduction in U will lead to gapless particle-hole excitations with same momentum.

For one added electron to the narrow upper band, the characteristic strong-coupling signature of multi-magnon processes and the large energy shift relative to the mean-

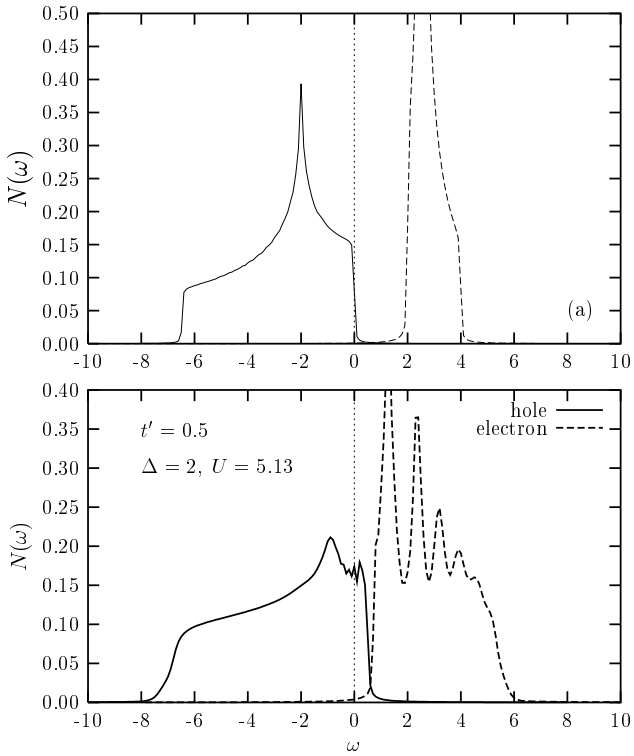


FIG. 14: Classical (a) and renormalized (b) one-particle density of states for one added hole and electron, showing the vanishing of the energy gap. The classical-level band asymmetry strongly influences the quantum corrections.

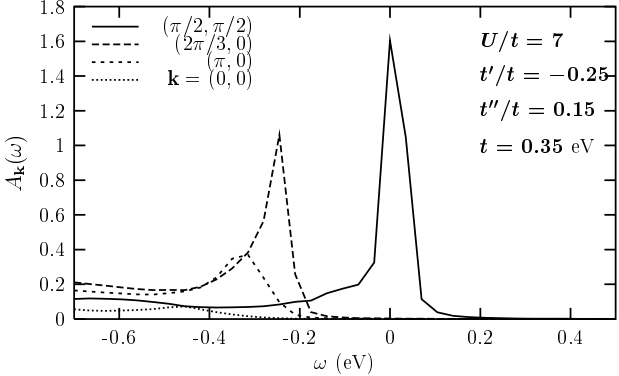


FIG. 15: Spectral function shows sharp quasiparticle peaks for $\mathbf{k} = (\pi/2, \pi/2)$ and $(2\pi/3, 0)$, as seen in photoemission experiments on cuprates.

field DOS confirms the strong fermion-magnon scattering associated with a narrow band. The pseudo-gap feature is also significantly enhanced. On the other hand, for one added hole to the wide lower band, significantly weaker fermion-magnon scattering is evident.

Taking the same cuprate parameters as obtained from a recent magnon spectrum fit,²² and including a small t'' term, we have obtained the spectral function for key

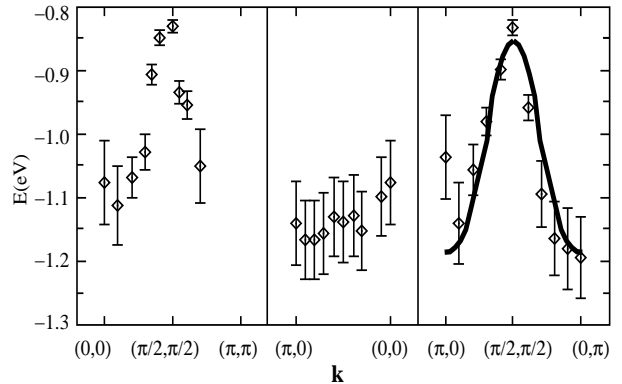


FIG. 16: Quasiparticle dispersion along $(\pi, 0) — (0, \pi)$ with same set of parameters as in Fig. 15, along with experimental ARPES data for $\text{Sr}_2\text{CuO}_2\text{Cl}_2$ from Ref. [2].

states and the quasiparticle dispersion along $(\pi, 0) — (0, \pi)$, as shown in Figs. 15 and 16. Excellent agreement with the photoemission experiments is obtained with regard to i) energy difference between $(\pi/2, \pi/2)$ and $(\pi, 0)$ states, ii) sharp peaks for $(\pi/2, \pi/2)$ and $(2\pi/3, 0)$, and iii) insignificant (low) spectral weights for $(0, 0)$ and $(\pi, 0)$ states. With the same NN hopping term $t = 0.35$ eV, our finite- U study yields $t' \approx -0.09$ eV and $t'' \approx 0.05$ eV, which are quite smaller than the $t - J$ model values ($t' \approx -0.12$ eV and $t'' \approx 0.09$ eV) of Ref. [3].

VI. CONCLUSIONS

We have obtained one-particle self-energy corrections in the AF state of the $t - t' - t''$ Hubbard model within a formally weak-coupling diagrammatic scheme in which all rainbow (noncrossing) diagrams are summed, representing multiple magnon emission and absorption processes. For the Hubbard model in the strong coupling limit, the self-energy expression is shown to reduce exactly to the SCBA result for the $t - J$ model, apart from a classical dispersion term absent in the $t - J$ model. That the many-body expansion scheme can be carried over to the strong-coupling limit, indicates its applicability in the full U range from weak to strong coupling. By comparing the Hubbard and $t - J$ model results, we have shown that the classical dispersion term has a significant effect on quasiparticle energy, mass, and weight, especially with increasing J , and indeed, some features of photoemission experiments on cuprates, such as vanishing spectral weight for $\mathbf{k} = (0, 0)$, find natural explanation within the Hubbard model results.

The Hubbard model study provides for a smooth interpolation between the strong and weak coupling limits. The importance of multi-magnon processes and string excitations in the antiferromagnet, manifested in pronounced oscillations in spectral function and density of states, gradually diminishes with decreasing U , and the

spectral function becomes increasingly coherent, the real part of self energy shows a dominant single-magnon contribution, and the DOS smoothly approaches the free-particle limit. For the Hubbard model, the one-particle density of states shows a finite band gap for all U values, and the ratio E_g^*/E_g^0 of the renormalized band gap and the classical (mean-field) gap is found to be nearly 1/2 for a broad range of U values in the intermediate coupling regime.

The role of fermion scattering states on quasiparticle renormalization due to fermion-magnon interaction is highlighted by the t' -induced asymmetry, leading to quite different self-energy corrections for the two AF bands. We find pronounced strong-coupling signature of multi-magnon processes for the narrow band, whereas the broad band exhibits significantly weaker renormalization.

For finite t' , we find that the AF band gap vanishes at a critical interaction strength U_c . For $U < U_c$, electron-hole pairs can be spontaneously excited due to band overlap, which will reduce the sublattice magnetization and hence the classical gap, and thus further increase the band overlap. A first-order AF insulator - PM metal transition is therefore expected at $U = U_c$. In three dimensions, the z^2 dependence of self energy suggests significantly stronger suppression of the AF band gap, which can yield a moderate U_c for even smaller t' value.

With the same set of cuprate parameters as obtained from a recent magnon spectrum fit,²² excellent agreement with ARPES data for $\text{Sr}_2\text{CuO}_2\text{Cl}_2$ is obtained, both with respect to quasiparticle weight as well as dispersion, effectively providing a unified description of magnetic and electronic excitations in cuprates. The t'' value required is only half of that obtained within the $t - J$ model study of Ref. [3], highlighting the role of the finite- U induced classical dispersion term $4J\gamma_{\mathbf{k}}^2$.

At finite temperature thermal excitation of magnons will enhance the self-energy correction, further decreasing the band gap and leading to, for $U > U_c$, a temperature driven first-order phase transition. An exploration of both quantum and thermal phase transitions from the AF insulator to the PM metal, as relevant for systems such as V_2O_3 , is thus possible from quasiparticle renormalization due to self-energy correction. For finite doping, magnon damping due to decay into intraband particle-hole excitations²⁴ will have a significant role on quasiparticle damping through the imaginary part of the fermion self energy. These consequences of finite temperature and doping are presently under study.

APPENDIX A: SELF ENERGY IN THE AF STATE

If $[\Sigma(\mathbf{k}, \omega)]$ represents the self-energy matrix in the two-sublattice basis, then in terms of the mean-field eigenvalue $E_{\mathbf{k}}^0$ and eigenvector $|\mathbf{k}\rangle = \begin{pmatrix} \alpha_{\mathbf{k}} \\ \beta_{\mathbf{k}} \end{pmatrix}$, the renormalized Green's function is given by

$$[G(\mathbf{k}, \omega)] = \frac{1}{[G^0(\mathbf{k}, \omega)]^{-1} - [\Sigma(\mathbf{k}, \omega)]} = \frac{|\mathbf{k}\rangle\langle\mathbf{k}|}{\omega - E_{\mathbf{k}}^0 - \Sigma_{\mathbf{k}}(\omega)}, \quad (\text{A1})$$

where expectation value of the self-energy matrix

$$\Sigma_{\mathbf{k}}(\omega) \equiv \langle \mathbf{k} | \Sigma(\mathbf{k}, \omega) | \mathbf{k} \rangle = (\alpha_{\mathbf{k}}^* \ \beta_{\mathbf{k}}^*) \begin{bmatrix} \Sigma_{AA} & \Sigma_{AB} \\ \Sigma_{BA} & \Sigma_{BB} \end{bmatrix} \begin{pmatrix} \alpha_{\mathbf{k}} \\ \beta_{\mathbf{k}} \end{pmatrix} \quad (\text{A2})$$

yields the self energy $\Sigma_{\mathbf{k}}(\omega)$ for state \mathbf{k} .

Quasiparticle dispersion, weight, and density of states can then be obtained from Eq. (A1) for the renormalized fermion propagator. The renormalized quasiparticle energy $E_{\mathbf{k}}^*$ is obtained by solving

$$\omega - E_{\mathbf{k}}^0 = \text{Re } \Sigma_{\mathbf{k}}(\omega), \quad (\text{A3})$$

and the quasiparticle weight is given by

$$Z_{\mathbf{k}} = \left[1 - \frac{\partial}{\partial \omega} \text{Re } \Sigma_{\mathbf{k}}(\omega) \right]_{\omega=E_{\mathbf{k}}^*}^{-1}. \quad (\text{A4})$$

In the absence of an intersection, the quasiparticle energy is obtained from the location of the peak in the spectral function

$$A_{\mathbf{k}}(\omega) = \frac{1}{\pi} \text{Im} \text{Tr}[G(\mathbf{k}, \omega)] = \frac{1}{\pi} \text{Im} \frac{1}{\omega - E_{\mathbf{k}}^0 - \Sigma_{\mathbf{k}}(\omega)}, \quad (\text{A5})$$

which also yields the density of states

$$N(\omega) = \frac{1}{\pi} \sum_{\mathbf{k}} \text{Im} \text{Tr}[G(\mathbf{k}, \omega)] = \sum_{\mathbf{k}} A_{\mathbf{k}}(\omega). \quad (\text{A6})$$

APPENDIX B: AF INSULATING STATE

Self-energy corrections are quite different for the (undoped) AF insulating state. For example, an existing electron in the lower band can scatter into the empty upper band states, however, an added hole cannot. To contrast these two cases, we examine the renormalization of states in the undoped AF, and obtain the quantum correction to ground state energy as a simple application. We consider the first-order self-energy diagrams shown in Fig. 17, both of which do not contribute in the doped case, and which represent (a) static correction to the mean-field potential due to the density correction, and (b) mixing between states of the two AF bands. An exact cancellation to leading order (U) is shown below. Although diagram (b) has been studied,^{25,26,39,40,41} this cancellation appears not to have been discussed earlier.

1. Strong coupling limit

The first-order Green's function correction due to diagram (b) yields one-loop quantum corrections to spin

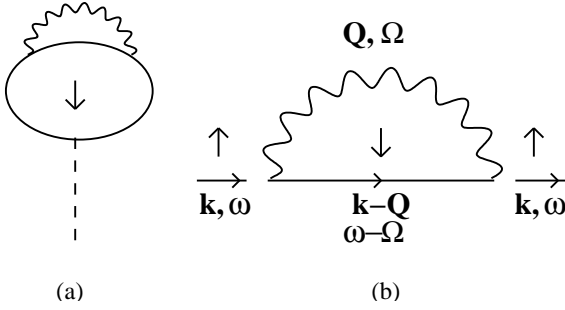


FIG. 17: First-order self-energy corrections, representing (a) correction to the mean-field (Hartree) energy and (b) mixing between states of the two AF bands.

densities and sublattice magnetization.²⁶ The spin- \downarrow density increases (decreases) on A (B) sublattice sites due to transfer of spectral weight from (to) the upper band. These density corrections of magnitude $\frac{1}{2} \sum_{\mathbf{q}} \left(\frac{1}{\sqrt{1-\gamma_{\mathbf{q}}^2}} - 1 \right)$ yield a self-energy correction

$$[\Sigma_{\uparrow}^{(a)}] = U[\delta n_{\downarrow}] = U \sum_{\mathbf{q}} \frac{1}{2} \left(\frac{1}{\sqrt{1-\gamma_{\mathbf{q}}^2}} - 1 \right) \begin{bmatrix} 1 & 0 \\ 0 & -1 \end{bmatrix} \quad (B1)$$

for diagram (a).

In diagram (b) representing mixing, for a state $|\mathbf{k} \uparrow\rangle$ in the lower (upper) band, and the intermediate state $|\mathbf{k} - \mathbf{q} \downarrow\rangle$ in the upper (lower) band, taking appropriate matrix elements of the fermionic and magnon propagators, we obtain the self-energy matrix for the lower band

$$[\Sigma_{\uparrow}^{(b)}(\mathbf{k}, \omega)]^{\ominus} = U^2 \frac{1}{2} \sum_{\mathbf{q}} \frac{1}{\omega - \Omega_{\mathbf{q}} - E_{\mathbf{k}-\mathbf{q}}^{\oplus} + i\eta} \times \begin{bmatrix} \left(1 - \frac{\epsilon_{\mathbf{k}-\mathbf{q}}^2}{U^2}\right) \left(\frac{1}{\sqrt{1-\gamma_{\mathbf{q}}^2}} - 1\right) & \left(\frac{\epsilon_{\mathbf{k}-\mathbf{q}}}{U}\right) \left(\frac{-\gamma_{\mathbf{q}}}{\sqrt{1-\gamma_{\mathbf{q}}^2}}\right) \\ \left(\frac{\epsilon_{\mathbf{k}-\mathbf{q}}}{U}\right) \left(\frac{-\gamma_{\mathbf{q}}}{\sqrt{1-\gamma_{\mathbf{q}}^2}}\right) & \left(\frac{\epsilon_{\mathbf{k}-\mathbf{q}}^2}{U^2}\right) \left(\frac{1}{\sqrt{1-\gamma_{\mathbf{q}}^2}} + 1\right) \end{bmatrix} \quad (B2)$$

and for the upper band

$$[\Sigma_{\uparrow}^{(b)}(\mathbf{k}, \omega)]^{\oplus} = U^2 \frac{1}{2} \sum_{\mathbf{q}} \frac{1}{\omega + \Omega_{\mathbf{q}} - E_{\mathbf{k}-\mathbf{q}}^{\ominus} - i\eta} \times \begin{bmatrix} \left(\frac{\epsilon_{\mathbf{k}-\mathbf{q}}^2}{U^2}\right) \left(\frac{1}{\sqrt{1-\gamma_{\mathbf{q}}^2}} + 1\right) & \left(\frac{-\epsilon_{\mathbf{k}-\mathbf{q}}}{U}\right) \left(\frac{-\gamma_{\mathbf{q}}}{\sqrt{1-\gamma_{\mathbf{q}}^2}}\right) \\ \left(\frac{-\epsilon_{\mathbf{k}-\mathbf{q}}}{U}\right) \left(\frac{-\gamma_{\mathbf{q}}}{\sqrt{1-\gamma_{\mathbf{q}}^2}}\right) & \left(1 - \frac{\epsilon_{\mathbf{k}-\mathbf{q}}^2}{U^2}\right) \left(\frac{1}{\sqrt{1-\gamma_{\mathbf{q}}^2}} - 1\right) \end{bmatrix}. \quad (B3)$$

These self-energy corrections have the formal structure of a second-order process involving mixing between states, and result in energy lowering (raising) for lower (upper) band states.

An exact cancellation to (leading) order U is seen between the Hartree shift $[\Sigma_{\uparrow}^{(a)}]$ of Eq. (B1) and the mixing

contributions $[\Sigma_{\uparrow}^{(b)}]$ of Eqs. (B2) and (B3), when the self energies $\Sigma_{\mathbf{k}\ominus}(\omega)$ and $\Sigma_{\mathbf{k}\oplus}(\omega)$ are evaluated from the corresponding matrices for the lower and upper bands, with $\omega = E_{\mathbf{k}}^{\ominus}$ and $E_{\mathbf{k}}^{\oplus}$, respectively, and the surviving terms of order J yield (for the lower band)

$$\begin{aligned} \Sigma_{\mathbf{k}\uparrow\ominus} = & \sum_{\mathbf{q}} \left(\frac{1}{\sqrt{1-\gamma_{\mathbf{q}}^2}} - 1 \right) \frac{\epsilon_{\mathbf{k}-\mathbf{q}}^2}{U} - \frac{\gamma_{\mathbf{q}}}{\sqrt{1-\gamma_{\mathbf{q}}^2}} \frac{\epsilon_{\mathbf{k}} \epsilon_{\mathbf{k}-\mathbf{q}}}{U} \\ & + J(1 - \sqrt{1 - \gamma_{\mathbf{q}}^2}). \end{aligned} \quad (B4)$$

The degeneracy in the classical (mean-field) dispersion along the magnetic zone boundary ($\epsilon_{\mathbf{k}} = 0$) is lifted by the first term in Eq. (B4). The $(\pi/2, \pi/2)$ state is pushed up more in comparison to the $(\pi, 0)$ state, because $\epsilon_{\mathbf{k}-\mathbf{q}}^2$ goes like $(\sin q_x + \sin q_y)^2$ and $(\cos q_x - \cos q_y)^2$, respectively, and therefore the small q contribution dominates for $\mathbf{k} = (\pi/2, \pi/2)$.

2. Ground-state energy

Due to mixing of states between the two bands, $[\Sigma_{\uparrow}^{(b)}(\mathbf{k}, \omega)]$ for a lower-band state yields spectral function in the upper band and vice-versa, resulting in transfer of spectral weight between the two AF bands. These modifications to the lower-band spectral function result in a quantum correction to the ground state energy, which we evaluate to first order from the corresponding correction to the Green's function.

While the coherent spectral weight in the lower AF band is reduced by $\frac{1}{2} \sum_{\mathbf{q}} \left(\frac{1}{\sqrt{1-\gamma_{\mathbf{q}}^2}} - 1 \right)$, an incoherent spectral function with identical integrated weight is transferred from the upper to the lower band. Focussing on the latter, for a state $|\mathbf{k}\oplus\rangle$, the first-order correction yields, to leading order,

$$\begin{aligned} [\delta G_{\uparrow}^{(1)}(\mathbf{k}, \omega)]_{BB} &= [\delta G_{\downarrow}^{(1)}(\mathbf{k}, \omega)]_{AA} \\ &= \frac{1}{2} \sum_{\mathbf{q}} \left(\frac{1}{\sqrt{1-\gamma_{\mathbf{q}}^2}} - 1 \right) \frac{1}{\omega + \Omega_{\mathbf{q}} - E_{\mathbf{k}-\mathbf{q}}^{\ominus} - i\eta}, \end{aligned} \quad (B5)$$

and the corresponding incoherent spectral function is

$$A_{\mathbf{k}}^{\text{incoh}}(\omega) = \frac{1}{2} \sum_{\mathbf{q}} \left(\frac{1}{\sqrt{1-\gamma_{\mathbf{q}}^2}} - 1 \right) \delta(\omega + \Omega_{\mathbf{q}} - E_{\mathbf{k}-\mathbf{q}}^{\ominus}). \quad (B6)$$

The first-order quantum correction $\delta E_{\mathbf{k}}^{(1)}$ to lower-band energy can thus be obtained by simply subtracting the mean-field contribution corresponding to the (coherent) spectral weight lost from the lower band, and adding the energy contribution of the (incoherent) spectral weight transferred to the lower band. With $E_{\mathbf{k}}^{\ominus} \approx$

$-\Delta - \epsilon_{\mathbf{k}}^2/U$, this yields

$$\begin{aligned}\delta E_{\mathbf{k}}^{(1)} &= -E_{\mathbf{k}}^{\ominus} \frac{1}{2} \sum_{\mathbf{q}} \left(\frac{1}{\sqrt{1 - \gamma_{\mathbf{q}}^2}} - 1 \right) + \int d\omega \omega A_{\mathbf{k}}^{\text{incoh}}(\omega) \\ &= -\frac{1}{2} \sum_{\mathbf{q}} \left(\frac{1}{\sqrt{1 - \gamma_{\mathbf{q}}^2}} - 1 \right) \left(\frac{\epsilon_{\mathbf{k}-\mathbf{q}}^2}{U} - \frac{\epsilon_{\mathbf{k}}^2}{U} + \Omega_{\mathbf{q}} \right).\end{aligned}\quad (\text{B7})$$

Summing over lower-band \mathbf{k} states for both spins yields

$$\delta E_g^{(1)} = \sum_{\mathbf{k}} \delta E_{\mathbf{k}}^{(1)} = -J \sum_{\mathbf{q}} \left(1 - \sqrt{1 - \gamma_{\mathbf{q}}^2} \right) \quad (\text{B8})$$

for the quantum correction to ground-state energy, which is exactly the spin-wave-theory result for the Heisenberg model.⁴² The net lowering in ground-state energy is thus a consequence of the incoherent spectral function in the lower band, spread over the magnon-energy scale.

* Electronic address: avinas@iitk.ac.in

- ¹ For recent reviews, see E. Dagotto, Rev. Mod. Phys. **66**, 763 (1994); A. Kampf, Phys. Rep. **249**, 219 (1994); W. Brenig, Phys. Rep. **251**, 153 (1995); M. A. Kastner, R. J. Birgeneau, G. Shirane, and Y. Endoh, Rev. Mod. Phys. **70**, 897 (1998).
- ² B. O. Wells *et al.*, Phys. Rev. Lett. **74**, 964 (1995).
- ³ C. Kim, P. J. White, Z.-X. Shen, T. Tohyama, Y. Shibata, S. Maekawa, B. O. Wells, Y. J. Kim, R. J. Birgeneau, and M. A. Kastner, Phys. Rev. Lett. **80**, 4245 (1998).
- ⁴ A. Nazarenko, K. J. E. Vos, S. Haas, E. Dagotto, and R. J. Gooding, Phys. Rev. B **51**, 8676 (1995).
- ⁵ V. I. Belinicher, A. I. Chernyshev, and V. A. Shubin, Phys. Rev. B **54**, 14914 (1996).
- ⁶ B. Kyung and R. A. Ferrel, Phys. Rev. B **54**, 10125 (1996).
- ⁷ T. Xiang and J. M. Wheatley, Phys. Rev. B **54**, R12653 (1996).
- ⁸ R. Eder, Y. Ohta, and G. A. Sawatzky, Phys. Rev. B **55**, R3414 (1997).
- ⁹ R. B. Laughlin, Phys. Rev. Lett. **79**, 1726 (1997).
- ¹⁰ T. K. Lee and C. T. Shih, Phys. Rev. B **55**, 5983 (1997).
- ¹¹ P. W. Leung, B. O. Wells, and R. J. Gooding, Phys. Rev. B **56**, 6320 (1998).
- ¹² A. V. Chubukov and K. A. Musaelian, J. Phys: Condens. Matter **7**, 133 (1995).
- ¹³ D. Duffy and A. Moreo, Phys. Rev. B **52**, 15607 (1995).
- ¹⁴ A. V. Chubukov and D. K. Morr, Phys. Rev. B **57**, 5298 (1998).
- ¹⁵ P. Bénard, L. Chen, and A. -M. S. Tremblay, Phys. Rev. B **47**, 589 (1993);
A. Veilleux, A. Daré, L. Chen, Y. M. Vilk, and A. -M. S. Tremblay, Phys. Rev. B **52**, 16255 (1995).
- ¹⁶ T. Tohyama and S. Maekawa, Phys. Rev. B **49**, 3596 (1993).
- ¹⁷ G. Stemmann, C. Pépin, and M. Lavagna, Phys. Rev. B **50**, 4075 (1994).
- ¹⁸ O. K. Andersen, A. I. Liechtenstein, O. Jepsen, and F. Paulsen, J. Phys. Chem. Solids **56**, 1573 (1995); E. Pavarini, I. Dasgupta, T. Saha-Dasgupta, O. Jepsen, and O. K. Andersen, Phys. Rev. Lett. **87**, 47003 (2001).
- ¹⁹ Z. X. Shen and D. S. Dessau, Phys. Rep. **253**, 1 (1995).
- ²⁰ H. H. Fretwell *et al.*, Phys. Rev. Lett. **84**, 4449 (2000).
- ²¹ S. V. Borisenko *et al.*, Phys. Rev. Lett. **84**, 4453 (2000).
- ²² R. Coldea, S. M. Hayden, G. Aeppli, T. G. Perring, C. D. Frost, T. E. Mason, S. -W. Cheong, and Z. Fisk, Phys. Rev. Lett. **86**, 5377 (2001).
- ²³ A. Singh and P. Goswami, Phys. Rev. B **66**, 092402 (2002).
- ²⁴ A. Singh and H. Ghosh, Phys. Rev. B **65**, 134414 (2002).
- ²⁵ A. Singh, cond-mat/0207032 (2002).
- ²⁶ A. Singh and Z. Tešanović, Phys. Rev. B **41**, 614 (1990).
- ²⁷ A. Singh, Phys. Rev. B **43**, 3617 (1991).
- ²⁸ S. Schmitt-Rink, C. M. Varma, and A. E. Ruckenstein, Phys. Rev. Lett. **60**, 2793 (1988).
- ²⁹ C. Gros and M. Johnson, Phys. Rev. B **40**, 9423 (1989).
- ³⁰ C. Kane, P. Lee, and N. Read, Phys. Rev. B **39**, 6880 (1989).
- ³¹ Z. Liu and E. Manousakis, Phys. Rev. B **44**, 2414 (1991); *ibid.* **45**, 2425 (1992).
- ³² F. Marsiglio, A. E. Ruckenstein, S. Schmitt-Rink, and C. M. Varma, Phys. Rev. B **43**, 10882 (1991).
- ³³ G. Martinez and P. Horsch, Phys. Rev. B **44**, 317 (1991).
- ³⁴ E. Dagotto *et al.*, Phys. Rev. B **41**, 9049 (1990).
- ³⁵ A. Singh, Phys. Rev. B **48**, 6668 (1993).
- ³⁶ P. Sen and A. Singh, Phys. Rev. B **48**, 15792 (1993).
- ³⁷ W. Brenig and A. Kampf, Europhys. Lett. **24**, 679 (1993).
- ³⁸ A. Singh, cond-mat/0006079 (2000); cond-mat/0112442 (2001).
- ³⁹ J. R. Schrieffer, X.-G. Wen, and S.-C. Zhang, Phys. Rev. B **39**, 11663 (1989).
- ⁴⁰ G. Vignale and M. R. Hedayati, Phys. Rev. B **42**, 786 (1990).
- ⁴¹ A. V. Chubukov and D. M. Frenkel, Phys. Rev. B **46**, 11884 (1992).
- ⁴² T. Oguchi, Phys. Rev. **117**, 117 (1960).